Minimizing Cost of Hierarchical OTN Traffic Grooming Boards in Metro Networks [Invited]

ARYANAZ ATTARPOUR[1,*], MEMEDHE IBRAHIMI[1], NICOLA DI CICCO[1], FRANCESCO MUSUMECI[1], ANDREA CASTOLDI[2], MARIO RAGNI[2], AND MASSIMO TORNATORE[1]

[1] *Department of Electronics, Information and Bioengineering, Politecnico di Milano, Milan, Italy*
[2] *SM-Optics, Cologno Monzese, Italy*
[*] *Corresponding author: aryanaz.attarpour@polimi.it*

Compiled September 13, 2023

Metro network operators aim to design scalable and cost-effective network architectures to address the capacity expansion due to ongoing traffic growth. While coherent transmission (at, e.g., 100 Gbps and 200 Gbps) is a solution to address capacity growth, operators must also still support legacy non-coherent transmission technology (at, e.g., 10 Gbps). Therefore, operators must devise new practical solutions to jointly support new and legacy transmission technologies, while minimizing network cost. In this study, we investigate the optimization problem arising when deploying a metro network with a hierarchical architecture of grooming nodes. More precisely, we optimize the deployment cost of hierarchical traffic-grooming stacked Optical Transport Network (OTN) boards with a mix of coherent and non-coherent transmission technologies in metro/regional networks composed of interconnected rings, while considering a filterless node architecture. We formulate the optimization problem using Integer Linear Programming. Then, to deal with problem scalability, we propose a comprehensive set of novel heuristic approaches based on Genetic Algorithms, Simulated Annealing, and a knowledge-domain heuristic (Local Search). We also compare the proposed approaches with baseline strategies used by network operators and show that we can reach up to 50% cost savings compared to these baselines.

http://dx.doi.org/10.1364/ao.XX.XXXXXX

1. INTRODUCTION

The increasing capacity demands brought on by *5G-and-beyond* applications require novel planning approaches for implementing low-cost network architectures [2, 4]. Serving all traffic demands at affordable network costs and ensuring that cutting-edge technologies are compatible with those already in use are some of the main challenges that network operators are currently facing. The adoption of coherent technologies has enabled supporting the need for high capacity and the adjustment of different configuration parameters to achieve improved network performance at the cost of a more complex network design. However, several network segments, including metro-access and metro-regional networks, still have a large base of legacy 10G non-coherent lightpaths that must be supported [1]. Therefore, to ensure cost-effective network planning, a hierarchical node architecture supporting co-existing coherent (100G/200G) and non-coherent (10G) transmission technologies is required [2]. In this paper, we investigate the optimization problem (referred to as minOTN) arising when deploying a metro network with grooming nodes characterized by a hierarchical architecture of grooming boards. Specifically, we optimize the deployment of hierarchical Optical Transport Network (OTN) traffic-grooming boards at the electrical layer, as well as coherent and non-coherent transponders and lightpath establishment at optical layer [3]. The intricacy of the problem is further increased when considering a combination of filtered and filterless node architecture in the optical layer. In particular, we assume that 2-degree nodes are filterless and higher-degree nodes are filtered, i.e., equipped with Wavelength Selective Switches (WSSs). Note that a filterless node is composed of passive splitters and combiners that replace WSSs [5–7]. The main benefits of filterless nodes are the low CapEx costs thanks to the replacement of costly WSSs, and low power consumption and footprint thanks to the low power requirements of passive equipment [17]. However, filterless nodes can lead to a higher spectrum consumption as a wavelength dropped at a node will propagate further due to the absence of WSSs. We have previously investigated the problem of minimizing the placement cost of OTN traffic-grooming boards in metro ring networks [2] and metro mesh networks [3]. This paper extends our previous work [3], where we considered the minOTN problem for optimizing the cost of deployment of OTN boards in mesh networks. We proposed two Genetic Algorithms (GA)-based approaches considering the k-shortest

path algorithm and the possibility of limiting the add & drop along the path. Compared to [3], the main novelties proposed in this paper are summarized as follows:

- We extended the ILP model to also include multi-degree nodes.
- We augmented the GA such that it can also consider smart initialization via user-defined heuristics.
- We propose new optimization approaches based on other metaheuristic algorithms (i.e., Simulated Annealing (SA)) and knowledge domain heuristics (i.e., Local Search (LS)).
- We ensure link-disjoint protection for traffic demands.

The remainder of this paper is organized as follows: In Section 2 we survey the state-of-the-art in traffic grooming in optical networks and we contextualize our work. In Section 3, we model the problem of minimizing OTN equipment deployment costs in mesh networks. Section 4 shows the ILP formulation of the problem. Section 5 introduces the approaches (i.e., GA, SA, LS, greedy heuristic) to solve the considered optimization problem. In Section 6, we describe illustrative case studies and report numerical results. Section 7 concludes our work.

2. RELATED WORK

The topic of how to build cost-effective optical metro networks has been recently revived, and it has been investigated under different criteria and aspects [8–10, 18]. In particular, traffic grooming is a main enabler for cost efficiency in optical metro networks, and it has been researched extensively in the last two decades [11–14]. Yet, most of existing work on traffic grooming investigates a conventional traffic-grooming problems without any consideration for support of mixed coherent and non-coherent transmission technologies as well as the hierarchical nature of the grooming boards. Most previous works have investigated the problem of minimizing the number of Add/Drop Multiplexers in ring networks. For example, authors in [15] considered minimizing the number of Add/Drop Multiplexers (ADMs) in ring networks using an ILP and simulated annealing. Also, in [16], authors minimize the cost of the network using the approximation algorithms, but the hierarchical nature of grooming boards is not considered. Furthermore, there are some studies that consider traffic grooming together with machine learning techniques. As an example, authors in [19] proposed a new approach based on machine learning techniques for traffic grooming in X-Haul. Moreover, on the topic of adaptive traffic grooming for Elastic Optical Networks (EON), authors in [20] proposed a traffic grooming approach on multilayer EON networks considering reinforcement learning.

In our recent work [2], for the first time, we considered the hierarchical traffic grooming problem together with the co-existence of 10G and 100G/200G lightpath in *metro ring* networks. We solved the minOTN problem by proposing an ILP model and a GA approach for filterless ring networks. Compared to [2], in this paper, we consider mesh networks with combined filtered, i.e., nodes equipped with WSSs, and filterless, i.e., nodes equipped with splitters and combiners, architectures. In addition, we consider path calculation based on the k-shortest path algorithm and constrain the number of Add & Drop steps performed between source and destination nodes. In conclusion, even though there exists a rich literature on traffic-grooming optimization problems in the last two decades, the traffic grooming problem investigated in this paper has not yet been explored, and, from the perspective of a vendor, the specific nature of this problem is extremely practical and very important.

3. *MinOTN* PROBLEM DESCRIPTION AND STATEMENT

In this section, first, we describe the node structure of network, then, we define the network structure and the interconnection of boards in the presence of traffic requests, and later we explain the problem statement and objective.

A. Node description

Figure 1 shows the hierarchical structure of a node composed of OTN boards, highlighting client interfaces and optical section of the node represented by the ROADM (Reconfigurable Optical Add Drop Multiplexer). A node consists of up to three stacked OTN boards: OTU2-ADM, OTU4-ADM, and OTU-TPD. Each node may be equipped with a pair (or more) of OTU2-ADM, OTU4-ADM, and OTU-TPD boards. In contrast to the assumptions in [2, 3] where we assumed that all boards need to be placed in pairs, here we consider that all OTN boards (OTU2-ADM, OTU4-ADM, OTU-TPD) can be deployed either as a single board or in pairs. Each OTU2-ADM board can support add & drop of traffic and perform multiplexing. Each OTU2-ADM has up to ten access interfaces, each with a maximum capacity of 10 Gbit/s, allowing clients to connect directly to the board. In addition, each OTU2-ADM board has four Small Form-factor Pluggable (SFP) interfaces that can be used as a 10 Gbit/s OTN point-to-point (p2p) line interface connecting to OTU4-ADM or a 10 Gbit/s OTN optical interface connecting to ROADM and capable of establishing a non-coherent 10G lightpath. If a 10G lightpath is established, a Dispersion Compensation Module (DCM) on each link and a channel filter at the receiver side should be placed. The OTU2-ADM board performs traffic grooming and aggregates clients' traffic into OTU2 signals sent to ROADM over non-coherent lightpaths or OTU4-ADM over black and white line connections. OTU4-ADM performs add & drop procedure and multiplexing, and clients can connect to OTU4-ADM boards through ten 10 Gbit/s access interfaces. Moreover, each OTU4-ADM board can receive/send traffic from/to OTU2-ADM via its four 10 Gbit/s line interfaces. OTU4-ADM can groom traffic of directly connected clients and OTU2-ADM into an OTU4 signal at the p2p line interface connected to an OTU-TPD board. Two OTU4-ADM boards can be connected as a pair and exchange traffic through a p2p interface with 100 Gbit/s capacity. An OTU-TPD board provides one OTN optical interface for at most two OTU4-ADM boards. OTU-TPD boards have two p2p line interfaces, each with 100 Gbit/s capacity, enabling the board to receive/send two OTU4 signals from/to different OTU4-ADM boards. In addition, these two interfaces can act as access interfaces enabling clients with 100 Gbit/s traffic to connect. An OTU-TPD has a colored output interface connected to a ROADM and establishes a coherent 100G/200G lightpath. The OTU-TPD board can aggregate clients/OTU4-ADM traffic into the established coherent lightpath.

B. Network description

In this section, we explain the interconnection of nodes in the network in the presence of traffic requests. As mentioned above, each node is equipped with OTN boards. Network nodes are connected through the links between their ROADMs. If there is a 10 Gbps traffic request between node i and node j, then the request can be routed through a 10G lightpath using the

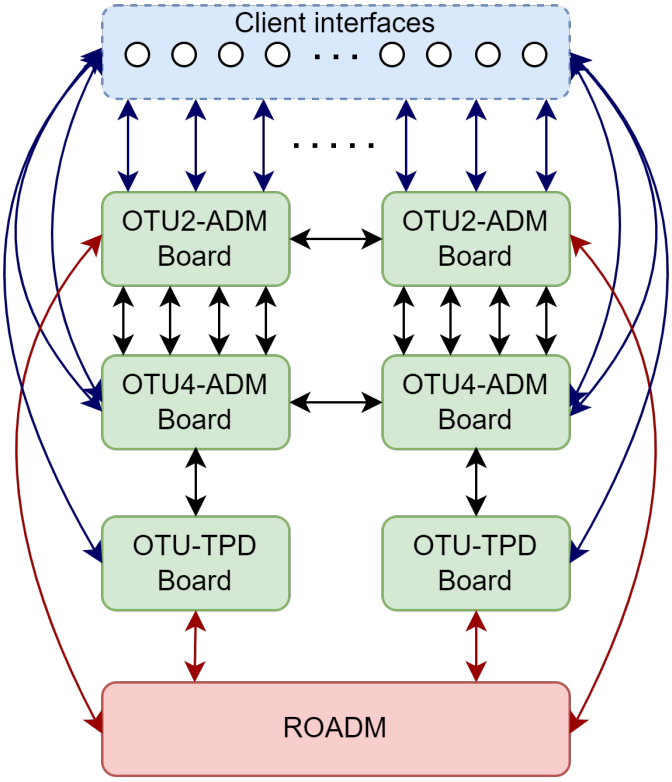

Fig. 1. Hierarchical node structure containing a pair of OTU2-ADM, OTU4-ADM, OTU-TPD boards, and a ROADM

OTU2-ADM boards of source-destination node pair. The request can also be routed through a 100G/200G lightpath using OTU2-ADM, OTU4-ADM and OTU-TPD boards. Note that 10 Gbps requests can also connect to OTU4-ADM directly and then continue to other nodes via 100G/200G lightpath using OTU-TPD boards. In all cases, the demand either can be routed through a direct lightpath between the source-destination pair, or it can be dropped in one or several intermediate nodes to groom with other demands. If traffic request is 100 Gbps, it connects to the OTU-TPD boards directly via the client interfaces and can go to the destination via a direct 100G lightpath, or it can be routed via 200G lightpath and dropped in one or several intermediate nodes to perform grooming.

C. Problem statement

The problem of deploying hierarchical OTN traffic grooming boards while minimizing equipment cost in mesh networks, namely *minOTN*, can be formally stated as follows: **Given** a mesh network topology, a set of traffic requests, a set of hierarchical OTN traffic grooming boards and interfaces as inputs, **Decide** the deployment of OTN boards and interfaces, routing, wavelength assignment and grooming of traffic requests by establishing coherent and non-coherent lightpaths with the **Objective** of minimizing the total cost of deployed equipment. The problem is **Constrained** by the capacity of the OTN boards and of the interfaces, fiber capacity in terms of number of wavelengths, and dedicated path protection for some of the traffic requests. In addition to the above, the problem is hard constrained by serving all the traffic demands. Note that we have not explicitly taken into account the spectrum usage in our objective function since we consider a filterless architecture. Moreover, in this aggregation network deployment, there is no fiber capacity filling. However, to ensure the optimization in the C-band, we consider the constraint of 40 lambdas per link.

4. INTEGER LINEAR PROGRAMMING (ILP) FOR minOTN PROBLEM

In [2], we developed an ILP model to minimize the cost of equipment in the minOTN problem for filterless horseshoe ring networks. In this paper, we extend the ILP model introduced in [2] for generic mesh networks. The main differences compared to the ILP in [2] are as follows:

- Compared to ring networks, in mesh networks nodes have different degrees. Nodes with degree larger than 2 are assumed to be equipped with WSS. Therefore, in the ILP model, we distinguish between nodes with degree equal to 2 and larger than 2, respectively. In the first type, the filterless constraints are kept, while in the second type, the filterless constraints are eliminated, as the nodes are assumed to be equipped with WSS. Filterless constraints are shown in Eq. (1-4). Eq. 1 and 2 indicate whether a wavelength w is used in a link (i,j). If the wavelength w is used, then λ_w is set to "1". If $\lambda_w = 1$, then all the colored links (i,j), i.e., $f_{i,j,w}$ are equal to "1" for w, meaning that wavelength w cannot be re-used. If wavelength w is broadcast on the link (i,j), then Eq. 3 and 4 require that bi,j,w be equal to 1.

$$M * \lambda_w \geq \sum_{(i,j)\in E_R} f_{i,j,w} \qquad \forall w \in W \qquad \textbf{(1)}$$

$$\sum_{(i,j)\in E_7 \cup E_6} f_{i,j,w} \leq 1 \qquad \forall w \in W \qquad \textbf{(2)}$$

$$b_{i,j,w} \leq \lambda_w * y_{i,j} - f_{i,j,w} \qquad \forall (i,j) \in E_R, w \in W \qquad \textbf{(3)}$$

$$b_{i,j,w} \geq \lambda_w * y_{i,j} - f_{i,j,w} \qquad \forall (i,j) \in E_R, w \in W \qquad \textbf{(4)}$$

- OTU-TPD boards are not constrained to be placed in pairs as in [2].

- Since we now consider traffic requests of 100 Gbps, we assume that each OTU-TPD board has two 100 Gbps interfaces to accommodate 100 Gbps demands from/to clients. These interfaces were not used in ring networks since the traffic distribution was between 1 Gbps and 10 Gbps. Eq. 5 shows the constraints on interfaces in OTU-TPD boards.

$$\sum_{(i,j)\in E3} y_{i,j} <= 2 \qquad \forall j \in N_3 \qquad \textbf{(5)}$$

- The new ILP model can route the demands by establishing 10G, 100G, and 200G lightpaths.

The objective function is expressed as minimizing the cost (μ) of logical nodes (δ), i.e., OTN boards and interfaces, and cost (ρ) of transponders ($\tau_{i,w}$) used to establish lightpaths on wavelength w, as follows:

$$\min \sum_{j\in N} \delta_j * \mu_j + \sum_{i\in N_3, w\in W} \tau_{i,w} * \rho_i \qquad \textbf{(6)}$$

In mesh networks with a relatively small number of nodes, the number of variables and constraints can reach millions. More

Table 1. Sets and subsets of ILP

N_{1AP}, N_{2AP}	Subset of logical nodes representing client interfaces of *OTU2-ADM* and *OTU4-ADM* boards
N	Set of logical nodes representing OTN boards and interfaces
N_1, N_2, N_3, N_4	Subset of logical nodes representing *OTU2-ADM*, *OTU4-ADM*, OTU-TPD boards and ROADMs
E	Set of links representing optical links and connection between interfaces of OTN boards
E_0	Subset of logical links representing connections of a client to interfaces of *OTU2-ADM* and *OTU4-ADM*
E_1, E_2	Subset of logical links representing connections to client interfaces to *OTU2-ADM*and *OTU4-ADM*, respectively
E_3	Subset of logical links representing connections of a client to interfaces of *OTU-TPD*
E_4	Subset of links representing the line interfaces between *OTU2-ADM* and *OTU4-ADM*
E_5	Subset of links representing the line interfaces between *OTU4-ADM* and *OTU-TPD*
E_6	Subset of links representing coherent colored interfaces between *OTU-TPD* and ROADM
E_7	Subset of links representing non-coherent colored interfaces between *OTU2-ADM* and ROADM
E_R	Subset of links representing links between ROADMs
W	Set of wavelengths
D	Set of connection requests (demands)
M	Assumed number

precisely, the number of variables of the ILP model is equal to $((1+W)(2E+ED+N+1)-1)$ and the number of constraints is equal to $(E_6+E_7+E_R)(2W+DW+D)+D(E_0^2+E_1^2+E_2^2+E_3^2+N+N_4+3N_4W+1)+2W(1+2E_R)+N_3(2+WE_6)+3N_1+N_2+2N_{1AP}+2N_{2AP}+5E+E_0+E_4+E_7$. Due to the complexity of the problem and limited scalability of the ILP, we need to rely on heuristic approaches to solve the problem, as discussed in the next section.

5. HEURISTIC STRATEGIES FOR THE *minOTN* PROBLEM

This section provides a description of the optimization strategies proposed to solve the minOTN problem. First, we describe the proposed metaheuristic approaches, i.e., GA and SA. Then, we show the greedy heuristic which is defined for fine-tuning the GA and SA. Later, we describe the LS approach, and in the last step, we explain the protection strategy that can be applicable to each of the approaches.

Table 2. Decision variables and parameters of ILP

$y_{i,j}$	Binary value equal to 1 if link *(i,j)* is activated/used
$\tau_{i,w}$	Binary variable equal to 1 if transponder i is activated and uses wavelength w
$f_{i,j,w}$	Binary variable equal to 1 if wavelength w is used in active link *(i,j)*
λ_w	Binary variable equal to 1 if wavelength w is used in the network (in any link $f_{i,j,w}$)
$b_{i,j,w}$	Binary variable equal to 1 if wavelength w is being broadcasted on link *(i,j)*
μ_j	Cost of logical node i, i.e., OTN board/interface
ρ_i	Cost of transponder i

A. Metaheuristics

To solve the minOTN problem through metaheuristics, we assume a path-based formulation. In particular, the input fed to GA and SA are sets of candidate source-destination paths to route and groom traffic requests. As such, we perform minOTN optimization in two steps: i) calculate a set of paths to route demands, and ii) GA and SA optimization considering paths from step 1 as inputs.

A.1. Path calculation

In the first step, the candidate paths need to be calculated for each demand from the source to the destination. Mesh networks are characterized by a high number of nodes. Therefore, calculating a set of paths between each source-destination pair leads to an excessive increase in complexity. To address this issue and reduce the number of paths between each source-destination pair, we consider the following approaches: i) we constrain the number of candidate paths by considering the k-shortest path algorithm, and ii) for mesh networks with a high number of nodes, we also limit the add & drop number in intermediate nodes [3]. An example of reducing the number of paths based on the k-shortest path algorithm and limiting the add & drop number is shown in Fig. 2. In Fig. 2.a, 3-shortest paths in number of hops from node 3 to node 4 are calculated. Then in Fig. 2.b and Fig. 2.c, the add & drop number along the shortest path is limited to m = 1 (m indicates the most number of possible add & drop in each node) meaning that the paths with more than one add & drop along them will be discarded like Fig. 2.d. Note that, since each node is equipped with OTN boards and we also consider the co-existence of the coherent and non-coherent transmission, based on the grooming options and capacity of each demand, the path for routing 10 Gbps (or less than 10 Gbps) demands can use the OTU2-ADM boards of the node pairs or can be routed through the OTU4-ADM and OTU-TPD boards and establish a 100G/200G lightpath. If the demand is 100 Gbps or more (less than 200 Gbps), it can be routed through the OTU-TPD boards of the node pairs and establish 100G/200G lightpath [2]. After path calculation, we provide these paths as inputs to the GA and the SA.

A.2. Genetic Algorithm

We developed a GA-based approach to solve the minOTN problem. An initial version of the GA-based approach for solving

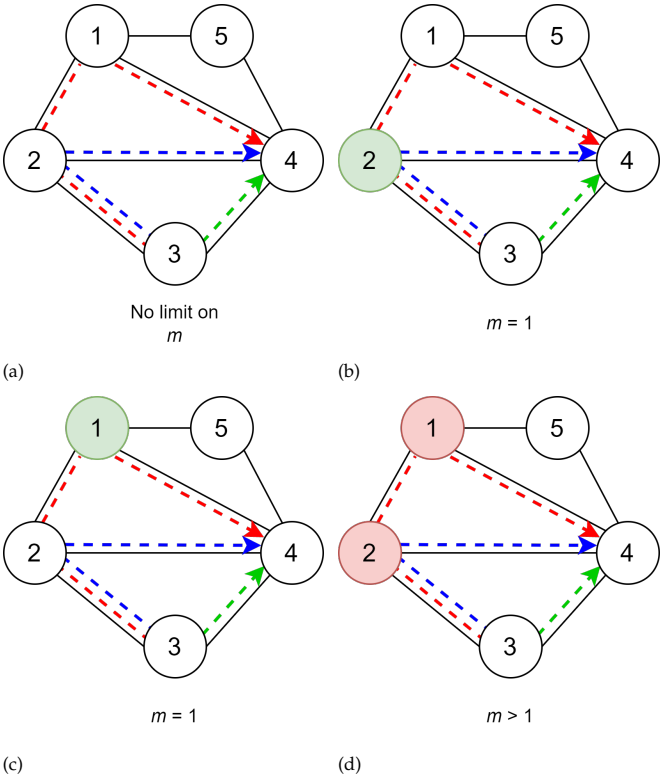

Fig. 2. a) Three shortest paths from node 3 to node 4. b,c) Limitation on the add & drop number is applied ($m = 1$). Add & drop is applied in green nodes successfully. d) Add & drop applied in two red nodes. Since $m = 1$, only paths with one or less than one add & drop are considered, and paths with more than one add & drop, like this path, will be discarded.

minOTN is provided in [3]. However, for the sake of completeness, we provide a complete description of the proposed approach in the following. The candidate source-destination path computed via the k-shortest-path algorithms are provided as inputs to the GA. The GA uses the calculated paths to generate the structure of genes, gene clusters, and chromosomes. Each chromosome represents a solution of the GA and it consists of multiple gene clusters, where each gene cluster consists of multiple genes. In our problem, the number of gene clusters is equal to the number of traffic demands and the number of genes in each gene cluster is equal to the number of candidate paths for the traffic demand that is represented by the gene cluster. The initial population of the GA is initialized either randomly or with an initial solution computed with a user-defined heuristic. After initialization, operations such as selection, crossover, and mutation are performed on members of the population, and then the next generation of solutions is generated [2]. The execution of the algorithm is terminated when a user-defined stopping condition is reached. In our case, we terminate the execution after *50*number of demands* generations after which the objective value is non-improving compared to the best solution found. Figure 3 represents the structure of GA containing chromosomes, gene clusters, and genes. In each chromosome, there are gene clusters as many as demands. Each gene cluster contains genes, and each gene stands for a candidate path for routing the demand. In each gene cluster, only one gene can be active, meaning that only one candidate path can be selected for routing the demand.

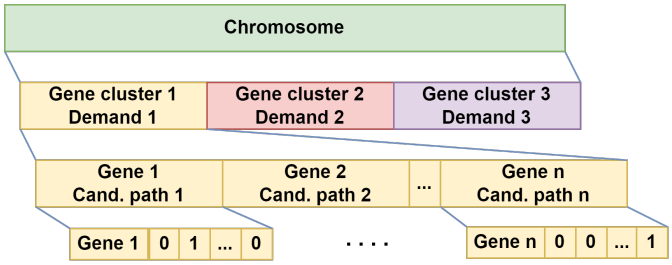

Fig. 3. GA structure: chromosome, gene clusters, and genes.

A.3. Simulated Annealing

An alternative strategy to solve minOTN is using an approach based on SA [21, 22]. SA is a metaheuristic based on a probabilistic method to approximate global optimization for a problem in a vast search space. In the context of minOTN problem, just like GA, SA uses the candidate paths as inputs of the problem. Therefore, the calculated candidate paths for routing and grooming demands (Section A.1) are given to the SA as input. Then, a multi-dimensional search space is used to formulate the SA based on candidate paths, in which each dimension corresponds to one traffic demand. The SA search space is depicted in Fig. 4, where each rectangle represents a dimension. The number of dimensions is equal to the number of traffic demands and each dimension contains the calculated candidate paths for routing that traffic demand. In Fig. 4, the calculated candidate paths for each dimension (traffic) are shown in each rectangle. The SA can start operating after specifying the search space and fine-tuning its parameters, such as the number of iterations, initial temperature, and temperature function. We introduce these parameters in the following sub-sections.

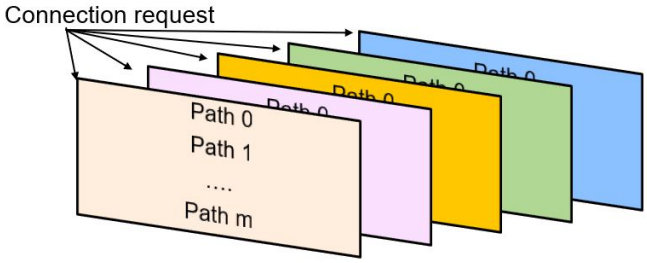

Fig. 4. The search space for SA. Each rectangle corresponds to a traffic demand (connection request (CR)); the paths for routing the demand are shown inside each rectangle.

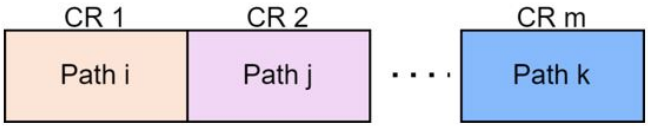

Fig. 5. A solution of the SA. For each CR (demand), a path is selected.

Number of iterations: SA aims to improve the solution of the minOTN problem in each iteration. The number of iterations to run the SA is a parameter of SA that also determines the stopping condition. The starting point of SA can be a randomly generated solution or a user-defined solution, e.g., defined based

on a heuristic algorithm. First, the SA randomly picks an initial solution. The solution of SA is one selected path for each dimension (traffic demand). Figure 5 depicts a solution of the SA. Then, the SA for the introduced solution checks the feasibility [2] and calculates the cost. The feasibility of a solution is defined as the number of passed constraints over the total number of constraints, while the cost of a solution is the sum of the cost of all deployed equipment (interfaces, boards, and transponders). In each iteration, the SA checks whether the total cost in this iteration is less than the previous iteration. If the cost in the new iteration is less than the cost in the previous one, the new solution will be substituted, and the new cost will be accepted. Otherwise, the SA can still accept the worse cost with a certain probability shown in Eq. 7, in which T_i is the temperature in each iteration. This procedure will continue until the maximum iteration number is reached.

$$P = \frac{1}{1 + exp(\frac{newcost - oldcost}{T_i})} \tag{7}$$

SA temperature function: The search in an SA-based approach depends on the definition of temperature. The temperature (T) is a parameter of SA that impacts the acceptance probability of the new solution. The SA starts from an initial temperature and decreases the temperature based on a pattern in each iteration. The initial temperature for solving the minOTN problem is set to 10000, and the pattern for reducing the temperature in each iteration follows the formula below:

$$T_i = \frac{T_0}{1 + a * \log(1 + i)} \tag{8}$$

T_i in Eq. 8 shows the temperature in each iteration, T_0 shows the initial temperature, and a is a constant number larger than one.

B. Greedy Heuristic

As mentioned above, the GA and the SA are by default initialized with randomly-generated solutions. For complex problems with large numbers of variables and constraints, like the minOTN problem, random initializations may overly inflate the computational times needed for convergence to good local optima. In contrast, providing good starting points for GA and SA can lead to solutions with better objective values and lower computational times, particularly for medium to large-size networks. In the following, we outline a simple but effective greedy heuristic for providing a smart initialization to our metaheuristic algorithms. We considered four different heuristics, and among them, we report only the heuristic with the best cost and we use it to initialize our GA and SA with it.

B.1. Heuristic: 100G direct-10G direct

The traffic demands in minOTN are either 10 Gbps or 100 Gbps. Our heuristic establishes 100G direct lightpaths from source to destination for routing 100 Gbps traffic demands and 10G direct lightpaths from source to destination for routing 10 Gbps traffic demands. This means that lightpaths do not drop in intermediate nodes, and an add & drop procedure has not been for the moment considered. Each 100G lightpath is established from the OTU-TPD board of the source node and drops in the OTU-TPD board of the destination node, whereas each 10G lightpath is established from OTU2-ADM of the source node and drops in OTU2-ADM of the destination node. Figure 6 illustrates an example of routing demands based on heuristic in 3-node network. There are 10 Gbps and 100 Gbps demands from node 1 to node 3. The heuristic routes 10 Gbps demand directly from the OTU2-ADM board of the source node to the OTU2-ADM board of the destination node via a 10G lightpath and routes 100 Gbps demands through a direct 100G lightpath using OTU-TPD boards of the node pairs. Note that in the example, only the used boards for routing are shown. Algorithm 1 shows the pseudocode of the proposed greedy heuristic. For each demand, If the demand is 10 Gbps, then a direct path based on k-shortest paths from the OTU2-ADM of source node to OTU2-ADM of destination node is selected for routing the demand. Otherwise, a direct path from the OTU-TPD of source node to OTU-TPD of destination node would be selected. Then the number of selected paths is given to GA as an initial point so that GA can start from the defined solution.

Algorithm 1. Pseudocode for greedy heuristic

```
Initializer_Vector← 0
for d ∈ D do
    if d is 10 Gbps or less then
        routes via direct 10G path← d
        Initializer_Vector← path
    else if d is 100 then
        routes via direct 100G path← d
        Initializer_Vector← path
GA← Initializer_Vector
```

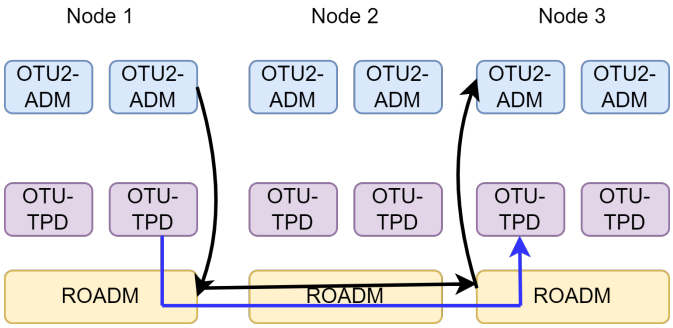

Fig. 6. Heuristic routes 10 Gbps and 100 Gbps demands through direct 10G (black) and 100G (blue) lightpaths.

C. Local Search

Another approach for solving the minOTN problem is based on LS. LS is a heuristic that explores a neighborhood of a given solution by performing local perturbation ("moves"), with the goal of improving the objective function value. The motivation behind developing the LS is using domain knowledge provided by domain experts to determine the "moves" of the local search in solving minOTN. To solve minOTN with LS, LS starts from the heuristic solution and tries to groom the 100 Gbps demands with the same source-destination node pair and route them through the 200G lightpath. Algorithm 2 indicates the pseudocode of the LS approach. LS takes the greedy heuristic solution as an initial solution. Then LS checks if there are 100 Gbps demands with the same source-destination pair to perform grooming and route the demands through a 200G lightpath. If there is cost reduction via grooming, LS accepts the new cost. Otherwise, it returns to the previous solution. If the demand is 10 Gbps, then it is routed through a direct 10G lightpath considering k-shortest paths from source to destination.

Algorithm 2. Pseudocode for Local Search

```
Init_Sol ← greedy_heuristic_solution
C ← LocalSearch(Init_Sol)
for d ∈ D do
    for d_i ∈ D do
        if d & d_i are 100G then
            Sol ← Groom d, d_i
            Ci ← LocalSearch(Sol)
            C ← Accept C_i if better than C
```

D. (1+1) dedicated protection for minOTN

In our solution, we also consider the protection of traffic requests. We assume a (1+1) link-disjoint protection, in which the working link is routed through the east side boards, and the backup link is routed through the west side boards and vice versa. In this case, first, we consider the k-shortest paths, and the working link is routed through the shortest path, and then the backup link is routed through the other side of the boards such that there are no common links between working and backup links. This protection strategy is applicable to all the mentioned approaches, and we consider the protection in all simulations that we report in Section 6. Figure 7 shows an example of the routing traffic requests through the shortest path: the working path is routed on the shortest path from the source node's east side to the destination node's west side. Therefore, to fulfill the link-disjoint constraint, the backup link is allocated from the source node's west side to the destination node's east side. Note that, for the sake of simplicity, only the used boards are shown in the example.

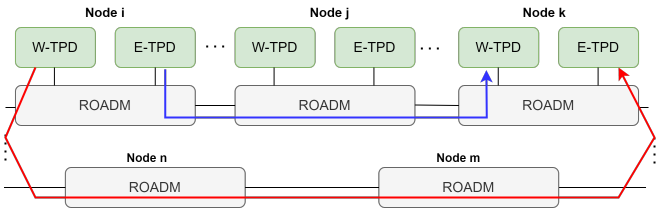

Fig. 7. The working path is routed through the blue path, and the backup link is routed through the red path.

E. Baseline strategy

This section introduces the baseline approach we consider for the minOTN problem. We assume that baseline approach supports only coherent transmission, meaning that traffic demands can be routed only through 100G/200G lightpaths. Therefore, if there is a 100 Gbps demand, the request will be routed through a direct 100G lightpath from the source to the destination. If the traffic demand is 10 Gbps, it will be routed through a 100 Gbps demand and will be dropped in the nodes with degrees more than two along the routing path. The reason for dropping and adding traffic requests in intermediate nodes with more than 2 degrees is to consider the possibility of grooming in hub nodes. If there are two 100 Gbps demands with the same source and destination, they will be groomed together and routed through the 200G lightpath.

6. ILLUSTRATIVE NUMERICAL RESULTS

This Section illustrates numerical results considering different mesh topologies, and for each topology, we report the cost of different approaches, i.e., ILP, GA, SA, LS, and baseline. First, we provide a description of evaluation settings, describing the adopted cost model and the topologies considered. Second, we show the validation of the proposed methodologies, i.e., GA, SA, and LS, compared to the optimal solution by the ILP. Finally, we provide the numerical results in a real-world 39-node network and compare our proposed solution with state-of-the-art baseline approaches.

A. Cost model

Figure 8 depicts the cost model and reports equipment cost, i.e., OTN board and interface costs, in cost units (cu). Equipment cost is provided by our industry partner and values are arbitrarily altered to preserve a confidential disclosure agreement. As shown in Fig. 8, the most expensive OTN board is the OTU-TPD board since it is equipped with transponder. The cost of a 200G transponder is higher than a 100G transponder. If the transponder establishes a 100G lightpath, the OTU-TPD board cost will be added for 5.0 cu. If the transponder establishes a 200G lightpath, the OTU-TPD board will be added for 6.12 cu. In addition to OTN boards and interfaces costs, if a 10G lightpath is established, a DCM (0.53 cu) on each link (one per direction), a filter (0.37cu) for each OTU2-ADM, and a channel filter (0.43 cu) at the receiver for each 10G lightpath are deployed. We consider common parts cost to represent the cost of a shelf where OTN boards are placed. Each shelf can host a pair of the same type of OTN boards, and if more boards are deployed, the cost is added accordingly.

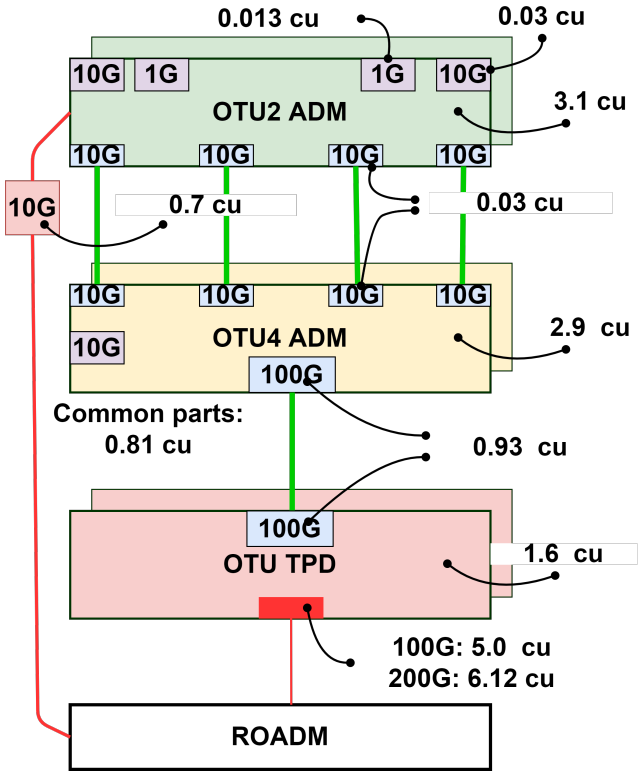

Fig. 8. The cost model shows the considered normalized cost for boards, interfaces, and transponders.

B. Validation with ILP

In this section, we validate the cost of our proposed approaches considering 5-node and 8-node mesh networks with the ILP model.

B.1. 5-node mesh network

Figure 9 illustrates the topology of a 5-node network. The green nodes are the nodes with WSS and the gray nodes are filterless nodes. The traffic is distributed as 10 Gbps, and 100 Gbps demands. The total considered traffic for this network is 720 Gbps, and around 20% of this amount is protected traffic. Table 3 reports the results of different approaches for this network. We report the average cost over five runs for the GA and the SA approaches and the best cost among them. All other approaches are deterministic, hence, the computed solution does not change over different runs.

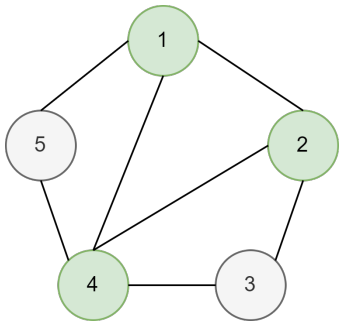

Fig. 9. 5-node network topology. Green nodes are the WSS nodes and the gray nodes are filterless nodes.

First, the 3-shortest paths are calculated and given to the GA without any limitation on the number of add & drop along the shortest paths. Later, we limit the number of add & drop to 2 ($m = 2$) and further to 1 ($m = 1$). All three GA-based approaches reached the exact cost as ILP in significantly less time compared to ILP. The LS also found the optimum cost in much less time compared to other approaches. Then, we report the cost of SA-based approaches. We start with calculating the k-shortest paths (k=3) without constrained add & drop and then fed the paths to the SA. Contrary to GA and LS approaches, the SA could not reach the ILP cost. To enhance the SA performance, one solution is to make the search space of SA smaller by reducing the number of paths by limiting add & drop along the shortest paths. Therefore, we consider $m = 2$. Reducing the number of routes results in an improvement in SA performance and the SA can achieve lower best cost and lower average cost compared to the without add & drop case, but not the ILP cost. Therefore, we further reduce the number of paths and consider $m = 1$, and the search space of the SA is even smaller, and this helps the SA to reach the same cost as ILP. As it is shown in Table 3, the proposed GA, SA ($m = 1$), and LS approaches can reach the same cost as ILP and have 51% cost savings compared to the baseline approach.

B.2. 8-node mesh network

This section considers the 8-node network. Figure 10 shows the topology of this network. The green nodes are equipped with WSS, and the gray nodes are the filterless nodes. The amount of traffic for this network is 540 Gbps. The distribution of demands is 10 Gbps and 100 Gbps and demands may be protected. Table 4 reports the best and average costs for the GA and the SA approaches and the cost for ILP, LS, and baseline. Like the 5-node network, first, the 3-shortest paths are calculated and fed to GA. All GA-based approaches (with or without add & drop limitation) can reach the ILP cost in significantly less time. Then, we consider the LS approach, which reached a cost slightly more than ILP (around 0.5%), but in significantly less time compared to all approaches. The other set of results relates to the SA-based approaches. First, the 3-shortest paths without constrained add & drop are calculated and given to the SA as input. The best cost and avg cost of SA are more than ILP cost. Therefore, there is a need to consider the limitation on the number of add & drop along the paths to reduce the search space and help the SA to converge better. First, the m equals 2 and the performance of SA in both best and avg cost is improved but still, the best cost is different from the ILP cost. Therefore, by considering m equals 1, the SA can reach the exact cost as ILP. The proposed approaches save up to 47% compared to the baseline.

Table 3. Cost minimization for 5-node network

Approach	Best Cost (cu)	Avg Cost (cu)	Avg Time
ILP	1741	-	$<$ 2 days
GA	1741	1741	$<$ 1 min
GA, m=2	1741	1741	$<$ 1 min
GA, m=1	1741	1741	$<$ 1 min
SA	2394	2522	1 min
SA, m=2	1859	1955	$<$ 1 min
SA, m=1	1741	1741	$<$ 1 min
LS	1741	-	1s
Baseline	3591	-	-

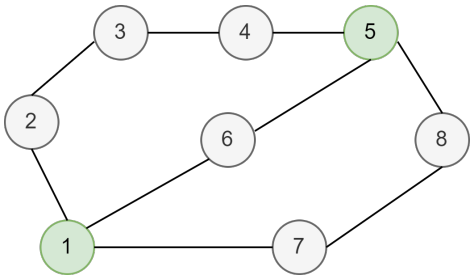

Fig. 10. 8-node interconnected ring mesh network topology. Green nodes are WSS nodes and the gray nodes are the filterless nodes.

C. 39-node mesh network

In this part, we consider a real-world 39-node mesh network with two different traffic matrices, and compare the results of different proposed approaches. The topology of the real 39-node mesh network is shown in Fig. 11. For this network, we consider two different traffic matrices. The first traffic matrix (TM1) has around 2 Tbps traffic distributed between 10 Gbps and 100 Gbps with ratio of 34% and 66% in terms of 10 Gbps and 100 Gbps demands and considering that 20% of demands are to be protected. Then, we consider the same network with an incremental traffic matrix compared to TM1. In particular, we increase the amount of traffic by 30% in TM2, distributed

Table 4. Cost minimization for 8-node network

Approach	Best Cost (cu)	Avg Cost (cu)	Avg Time
ILP	1614	-	$<$ 1 day
GA	1614	1614	$<$ 1 min
GA, m=2	1614	1614	$<$ 1 min
GA, m=1	1614	1614	1 min
SA	2227	2829	$<$ 3 min
SA, m=2	1636	1650	$<$ 1 min
SA, m=1	1614	1614	1 min
LS	1622	-	1s
Baseline	3094	-	-

among 10 Gbps demands (15%) and 100 Gbps demands (15%). The ratio between 10 Gbps and 100 Gbps demands is 44% and 56%, repectively, and 30% of demands are protected.

C.1. 39-node network with TM1

Considering mesh networks with a high number of nodes increases the possibility of choices in routing and grooming. Accordingly, the number of candidate paths increases, and it would be time-consuming to calculate all these paths. Consequently, calculating paths for the GA and the SA without any add & drop limitation will take too much time and will not be scalable. Therefore, we reduce the number of paths by constraining the number of add & drop along the paths for both the GA and the SA. Since some of the traffic demands are protected, due to the large scale of the network, we calculated the 5-shortest paths instead of the 3-shortest paths to fulfill the link-disjoint protection. Table 5 reports the cost of different approaches. The GA-based approaches find the same best cost when the number of add & drop is $m = 1$ and $m = 2$. The average cost when m equals 2 is slightly more than the case in which m equals 1. The reason is that the search space of GA when $m = 1$ is smaller, and the GA can converge to the same cost in each run. Then, we check the SA-based approaches. As shown in Table 5, the best cost of SA when $m = 2$ is far from the best cost of GA. The best cost of SA improves when the $m = 1$, and the reason is smaller search space. However, the cost of SA when $m = 1$ is still more than the best cost of GA. Therefore, we decide to initialize our SA with the heuristic solution and repeat the simulation. It is obvious that starting from the wise initial point instead of the random one helped the SA to improve the cost and find a better solution. In the case that SA is initialized with the heuristic and the $m = 2$ compared to the case that SA is initialized randomly, and $m = 2$, we see almost 40% cost reduction. We also can see the improvement in the SA performance when it is initialized with heuristic and $m = 1$ compared to the random initialized SA with $m = 1$. The LS cost is the same as the heuristic initialized SA cost with $m = 1$ and it is close to the cost of GA (0.5% more than GA cost). The only difference between the GA and the SA-In. with $m = 1$ and LS is in the number of common parts. The GA solution placed less number of common parts compared to LS and SA.In. with $m = 1$. The GA, SA, and LS have cost savings of up to 53% compared to the baseline. Note that the ILP is unable to find the optimal solution for 39-node networks.

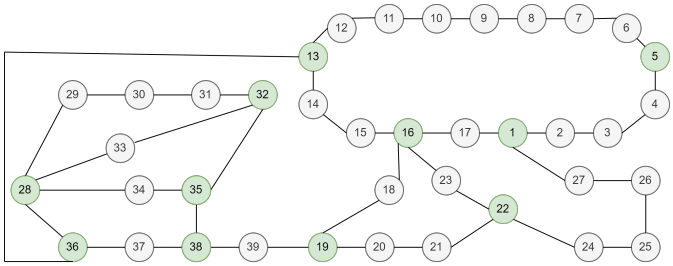

Fig. 11. 39-node interconnected ring mesh network topology. Green nodes are WSS nodes and gray nodes are filterless nodes.

Table 5. Cost minimization for 39-node network with TM1

Approach	Best Cost (cu)	Avg Cost (cu)	Avg Time
ILP	N.A.	-	-
GA	N.A.	-	-
GA, m=2	5996	6002	$<$ 1 min
GA, m=1	5996	5996	1 min
SA	N.A.	-	-
SA, m=2	10600	11026	6 min
SA, m=1	6374	6570	4 min
SA-In., m=2	6503	6503	5 min
SA-In., m=1	6028	6028	3.7 min
LS	6028	-	1s
Baseline	13003	-	-

C.2. 39-node mesh network with TM2

In this part, we report the results of the same network with TM2. The ILP model is not scalable for this network. Furthermore, calculating the number of paths without considering the limitation of add & drop for the GA and the SA approaches with such a high number of traffic demands is not scalable. Therefore, we start with the GA-based approaches with add & drop limitation in Table. 6. The best cost of GA with $m = 1$ is less than that of GA with $m = 2$. The reason is better convergence of GA when the search space is smaller. Considering the SA-based approaches, the best cost of SA with $m = 1$ is much less compared to $m = 2$, but still far from the best cost of GA. We initialize the SA with the heuristic solution to enhance the SA approaches. The initialized SA with $m = 1$ and $m = 2$ reached the same cost. The initialized SA also achieved a better best cost than the GA with $m = 2$. The cost of LS is as same as the cost of initialized SA with $m = 1$. The difference between the LS and GA costs is due to the number of common parts. Compared to the baseline, the proposed solutions can save up to 53%. Note that the increase in time is due to fine-tuning the algorithms and increasing the stopping condition with respect to the network scale.

7. CONCLUSION

In this paper, we solved the problem of minimizing the cost of OTN boards (minOTN) by considering different stacked OTN boards and hierarchical traffic grooming in mesh networks. We

Table 6. Cost minimization for 39-node network with TM2

Approach	Best Cost (cu)	Avg Cost (cu)	Avg Time
ILP	N.A.	-	-
GA	N.A.	-	-
GA, m=2	8583	8684	10 min
GA, m=1	8399	8402	7 min
SA	N.A.	-	-
SA, m=2	17701	18100	21 min
SA, m=1	10813	11074	8 min
SA-In., m=2	8455	8455	15 min
SA-In., m=1	8455	8455	7 min
LS	8455	-	1s
Baseline	18408	-	-

also consider the co-existence of coherent and non-coherent transmission technologies and filterless architecture. We proposed different approaches based on the GA, SA, and LS algorithms. In addition, we developed an ILP model to verify the optimization of proposed models. We tested our approaches on two small networks and showed that our proposed approaches can find the optimal solution in much less time compared to ILP. Later, we considered a real mesh network with two different traffic matrices and showed that our proposed approaches can be reached up to 50% cost savings compared to the baseline approach. As future work, we plan to solve the minOTN problem while considering an accurate physical layer modeling that captures transmission impairments when deploying mixed transmission technologies such as coherent and non-coherent. We plan to consider both linear and nonlinear impairments of signal transmission as well as penalties such as insertion and filtering losses.

Table 7. Acronyms

ILP	Integer Linear Programming
GA	Genetic Algorithm
SA	Simulated Annealing
LS	Local Search
SA-In.	Simulated Annealing with heuristic initialization
ROADM	Reconfigureable Optical Add Drop Multiplexer
OTN	Optical Transport Network
OTU2-ADM	Optical Transport Unit2-Add Drop Mulitplexer
OTU4-ADM	Optical Transport Unit4-Add Drop Mulitplexer
OTU-TPD	Optical Transport Unit-Transponder
DCM	Dispersion Compensation Module
WSS	Wavelength Selective Switch
ADM	Add Drop Multiplexer
N.A.	Not Applicable

REFERENCES

1. E. Virgillito, *et al.*, "Experimental Validation of QoT Computation in Mixed 10G/100G Networks." ACP Conference, 2021.
2. M. Ibrahimi, *et al.* Minimizing equipment and energy cost in mixed 10G and 100G/200G filterless horseshoe networks with hierarchical OTN boards. Ann. Telecommun. (2022).
3. A. Attarpour, *et al.* "Minimizing Cost of Hierarchical OTN Traffic Grooming Boards in Mesh Networks," GLOBECOM 2022 - 2022 IEEE Global Communications Conference, Rio de Janeiro, Brazil, 2022, pp. 3700-3705.
4. O. Karandin, *et al.*, "Optical Metro Network Design with Low Cost of Equipment," 2021 International Conference on Optical Network Design and Modeling (ONDM), Gothenburg, Sweden, 2021, pp. 1-4.
5. O. Karandin, *et al.*, A techno-economic comparison of filterless and wavelength-switched optical metro networks," in International Conference of Transparent Optical Networks, (2020), pp. 1–4.
6. C. Tremblay *et al.*, "Agile optical networking: Beyond filtered solutions", Proc. Opt. Fiber Commun. Conf., pp. 1-3, 2018
7. M. Ibrahimi, *et al.*, "Strategies for Dedicated Path Protection in Filterless Optical Networks," 2021 IEEE Global Communications Conference (GLOBECOM), Madrid, Spain, 2021, pp. 01-06.
8. M. Ibrahimi *et al.*, "QoT-Aware Optical Amplifier Placement in Filterless Metro Networks," in IEEE Communications Letters, vol. 25, no. 3, pp. 931-935, March 2021.
9. de Sousa, Léia Sousa, and André C. Drummond. "Metropolitan optical networks: A survey on single-layer architectures." Optical Switching and Networking (2022): 100719.
10. M. M. Hosseini, J. Pedro, A. Napoli, N. Costa, J. E. Prilepsky and S. K. Turitsyn, "Long-Term Cost-Effectiveness of Metro Networks Exploiting Point-to-Multipoint Transceivers," 2022 International Conference on Optical Network Design and Modeling (ONDM), Warsaw, Poland, 2022, pp. 1-6.
11. R. Dutta, *et al.*, "Traffic grooming for optical networks: foundations, techniques and frontiers," in Springer Science & Business Media, 2008.
12. B. Mukherjee, I. Tomkos, M. Tornatore, P. Winzer, and Y. Zhao, "Springer Handbook of Optical Networks," in Springer Nature, 2020.
13. Keyao Zhu and B. Mukherjee, "Traffic grooming in an optical WDM mesh network," in IEEE Journal on Selected Areas in Communications, vol. 20, no. 1, pp. 122-133, Jan. 2002.
14. Zhang, Jiawei, *et al.*, "Dynamic traffic grooming in sliceable bandwidth-variable transponder-enabled elastic optical networks." Journal of Lightwave Technology 33.1 (2015): 183-191.
15. J. Wang, *et al.*, "Improved Approaches for Cost-effective Traffic Grooming in WDM Ring Networks: Nonuniform Traffic and Bidirectional Ring," in IEEE/OSA JLT, vol. 19, no. 11, pp. 1645-1653, 2001.
16. M. Flammini, *et al.*, "The Traffic Grooming Problem in Optical Networks with Respect to ADMs and OADMs: Complexity and Approximation," in Algorithms, vol. 14, no. 5, pp. 1-12, 2021.
17. O. Ayoub, *et al.*, "Tutorial on filterless optical networks [Invited]," J. Opt. Commun. Netw. 14, 1-15 (2022).
18. João Pedro, Nelson Costa, and Steve Sanders, "Cost-effective strategies to scale the capacity of regional optical transport networks," J. Opt. Commun. Netw. 14, A154-A165 (2022).
19. J. Zhang, *et al.*, "ADMIRE: collaborative data-driven and model-driven intelligent routing engine for traffic grooming in multi-layer X-Haul networks," J. Opt. Commun. Netw. 15, A63-A73 (2023).
20. T. Tanaka, "Adaptive Traffic Grooming Using Reinforcement Learning in Multilayer Elastic Optical Networks," 2023 Optical Fiber Communications Conference and Exhibition (OFC), San Diego, CA, USA, 2023, pp. 1-3.
21. Kirkpatrick, S., Gelatt Jr, C.D. and Vecchi, M.P., 1983. Optimization by simulated annealing. science, 220(4598), pp.671-680.
22. Aarts, E. and Korst, J., 1989. Simulated annealing and Boltzmann machines: a stochastic approach to combinatorial optimization and neural computing. John Wiley & Sons, Inc.